Chin. Phys. Lett. **39**, 038201 (2022)

Probing the Air Storage Failure Mechanism of Ni-Rich Layered Cathode Materials

Qingyu Dong(董庆雨)[1†], Ruowei Yi(易若玮)[1†], Jizhen Qi(齐楫真)[1], Yanbin Shen(沈炎宾)[1*], and Liwei Chen(陈立桅)[2*]

[1]*i-Lab, CAS Center for Excellence in Nanoscience, Suzhou Institute of Nano-Tech and Nano-Bionics (SINANO), Chinese Academy of Sciences (CAS), Suzhou 215123, China*

[2]*In Situ Center for Physical Sciences, School of Chemistry and Chemical Engineering, Shanghai Jiaotong University, Shanghai 200240, China*

(Received 4 January 2022; accepted 26 January 2022; published online 1 March 2022)

Ni-rich layered oxide cathode materials, such as $LiNi_{0.83}Co_{0.12}Mn_{0.05}O_2$ (NCM811), exhibit high specific capacity and low cost, and become cathode material preference of high-energy-density Li-ion batteries. However, these cathode materials are not stable and will form Li-poor reconstructed layers and alkaline compounds (Li_2CO_3, LiOH) on the surface during the storage and processing in humid air, resulting in serious deterioration of electrochemical properties. During the past two decades, the consensus on the surface instability mechanism during humid air storage has not been reached. The main controversy focuses on the unstable octahedron mechanism and the Li/H exchange mechanism. Herein, we investigate the instability mechanism in the humid air by conducting scanning electronic microscopy, scanning transmission electron microscopy, and x-ray photoelectron spectroscopy analysis on NCM811 samples stored in designed atmospheres, etc., and realize that the surface instability of the NCM811 during storage should be mainly originated from Li/H exchange when it contacts with moisture.

DOI: 10.1088/0256-307X/39/3/038201

Li-ion batteries (LIBs) have been widely applied in fields such as portable devices and electric vehicles due to merits including high energy density, high operation potential, long cycle life, and limited environmental impact.[1,2] Ni-rich layered oxides $LiNi_xCo_yMn_{1-x-y}O_2$ ($x \geq 0.8$) are considered as a kind of most promising cathode materials for high energy density LIBs for their high specific capacity and low cost.[3,4] Typically, $LiNi_{0.8}Co_{0.1}Mn_{0.1}O_2$ (NCM811) receives much attention for its high practical specific capacity of more than $200\,mA{\cdot}h{\cdot}g^{-1}$.[5–7]

Due to the minimized Co content, the raw material cost of NCM811 is considerably lower than that of Co-rich cathode materials.[8,9] Nevertheless, the increased Ni content results in the air-storage and processing instability, which requires an ultradry environment from electrode fabrication to battery packaging.[10] This harsh environment control offsets the cost advantage of NCM811. Addressing this issue will benefit NCM811 in regaining its competitiveness against other cathode materials.[11] However, consensus has not been reached on the mechanism behind this air instability, which is unfavorable for the air stability amelioration.[12] During the past 20 years, controversy mainly focused on two points: (1) Due to the poor chemical stability of Ni^{3+} in the O^{2-} octahedron of the Ni-rich layered oxides, Ni^{3+} tends to be spontaneously reduced to Ni^{2+} and forms active oxygen species, which react to the adsorbed H_2O and CO_2 on the surface of Ni-rich cathode, and the lattice Li^+ on the inner surface of the material, forming LiOH and Li_2CO_3. Consequently, the inner surface of the oxide transforms from layered phase to Li-poor phases. The detailed process is expressed by the following former four reaction equations. This opinion hereafter is named as the unstable octahedron mechanism.[10,13–15] (2) The second failure mechanism is based on the Li/H exchange process, as illustrated by the following latter four reaction equations.[16–18] When the Ni-rich layered oxides are exposed to moisture, H^+ will exchange with the lattice Li^+ on the surface layer and substitute the Li^+ site, while the Li^+ meets the OH^- in water and results in the LiOH precipitation on the surface. The LiOH will be further transformed into Li_2CO_3 in contact with CO_2 in air. Due to the substitution of H^+, the surface of the NCM811 transforms into the metastable NiOOH phase, and then finally becomes the stable NiO-like rock-salt phase and releases O_2.

$$Ni^{3+} + O^{2-}_{(lattice)} \rightarrow Ni^{2+} + O^-, \quad (1)$$

$$O^- + O^- \rightarrow O^{2-}_{(active)} + O, \quad (2)$$

$$O^{2-}_{(active)} + CO_2 \rightarrow CO_3^{2-}, \quad (3)$$

†Qingyu Dong and Ruowei Yi contributed equally to this work.

*Corresponding author. Email: ybshen2017@sinano.ac.cn; lwchen2008@sinano.ac.cn

© 2022 Chinese Physical Society and IOP Publishing Ltd

$$O^{2-}_{(active)} + H_2O \rightarrow 2OH^-, \quad (4)$$

$$Li^+_{NCM} + H_2O \rightarrow H^+_{NCM}(MOOH) + Li^+ + OH^-, \quad (5)$$

$$MOOH \rightarrow \frac{1}{3}M_3O_4 + \frac{1}{2}H_2O + 1/12O_2, \quad (6)$$

$$M_3O_4 \rightarrow 3MO + \frac{1}{2}O_2, \quad (7)$$

$$2LiOH + CO_2 \rightarrow Li_2CO_3 + H_2O. \quad (8)$$

To clarify the actual failure mechanism behind the air instability, we herein design six groups of comparing experiments and conclude that the Li/H exchange process is the primary factor causing the formation of Li-poor reconstructed layer and alkaline compounds (Li_2CO_3, LiOH) on the surface of NCM811.

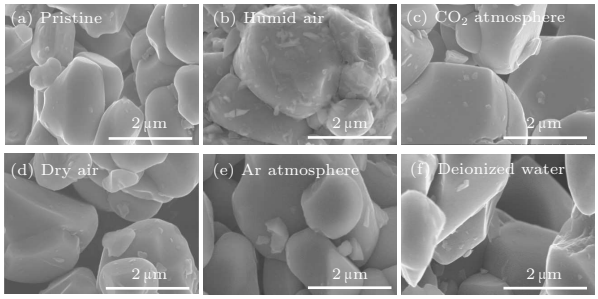

Fig. 1. The scanning electronic microscope (SEM) observation of NCM811 stored under different atmospheres. (a) The pristine NCM811 and the NCM811 stored (b) in humid air for 30 days, (c) in CO_2 for 60 days, (d) in dry air for 1 year, (e) in Ar for 1 year, and (f) after wash with deionized water.

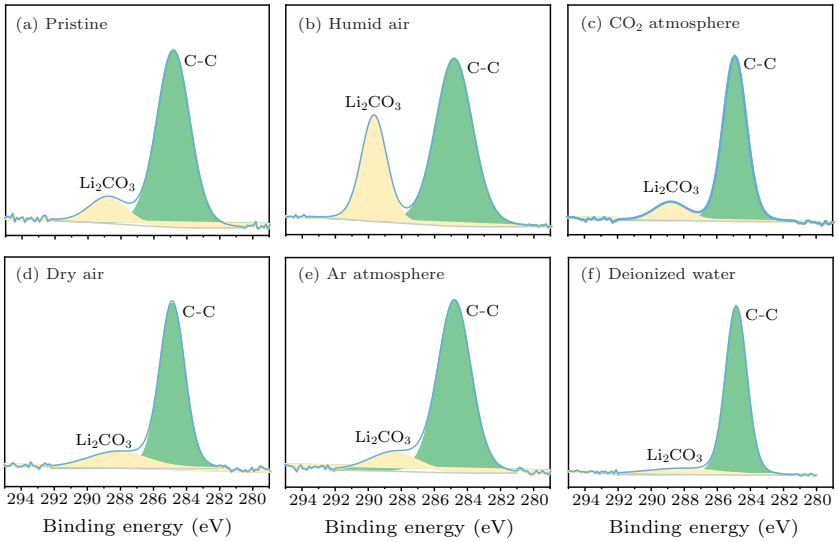

Fig. 2. The deconvoluted XPS C 1*s* spectra of (a) the pristine NCM811 and NCM811 stored (b) in humid air for 30 days, (c) in CO_2 for 60 days, (d) in dry air for 1 year, (e) in Ar for 1 year, and (f) after wash with deionized water. XPS: x-ray photoelectron spectroscopy.

Figure 1 and Fig. S1 in the Supplementary Material are the scanning electronic microscopy (SEM) images of pristine NCM811 and NCM811 stored at different atmospheres. Only the NCM811 in stored humid air for 30 days exhibits massive flake-like impurities on the surface [Figs. 1(b) and S1(b)], while other samples show no prominent difference surface morphology compared with the pristine one. The analysis of the surface chemistry is conducted through x-ray photoelectron spectroscopy (XPS), which is a surface-sensitive technology for qualitatively detecting the small amount of Li_2CO_3 on the NCM811 surface. Figures 2 and S2 show the deconvoluted C 1*s* (Li_2CO_3, 289.5 eV) and O 1*s* (Li_2CO_3, 531.5 eV) spectra of the pristine NCM811 and NCM811 samples stored in different atmospheres.[19,20] The area of the fitting peaks can be used to semi-quantitatively analyze the content of the Li_2CO_3. Due to the excessive Li source (LiOH) addition in the NCM811 synthesis process, a small amount of Li_2CO_3 and LiOH forms on the NCM811 surface after exposure to air, which can be removed by washing with deionized water. Therefore, a small amount of Li_2CO_3 can be detected on the pristine NCM811 [Fig. 2(a)] but almost no Li_2CO_3 can be detected on the one washed with deionized water [Fig. 2(f)]. Meanwhile, other samples stored in different atmospheres exhibit similar spectra with the pristine one except for the sample stored in the humid air, which presents prominent Li_2CO_3 generation [Fig. 2(b)].

Conclusions can be derived from the SEM and XPS results: Li_2CO_3 only generates on the NCM811 surface that is exposed to H_2O and CO_2 simultaneously and does not grow on samples stored in dry air (trace H_2O and CO_2) for 1 year or pure CO_2 atmosphere for 60 days. If the Li_2CO_3 formation is caused by the unstable octahedron mechanism, the NCM811 samples stored in pure CO_2 and dry air atmospheres will also generate Li_2CO_3 on the surface, which is contrary to the SEM observation and the XPS results [Figs. 1(c)

and 1(d)]. Therefore, these results do not support the unstable octahedron mechanism.[10,13]

Humid air storage not only brings Li_2CO_3 and LiOH on the NCM811 surface, but also reconstructs crystal structure and produces Li-poor phases on the particle surface. This surface structure reconstruction of NCM811 is verified by the scanning transmission electron microscopy (STEM) characterization, as shown in Figs. 3 and S3. It is evidenced by the STEM results that the disordered Li-poor phase is only induced on samples that contacts moisture (stored in humid air and washed with deionized water). On the contrary, NCM811 samples stored in pure CO_2 for 60 days and in dry air for 1 year exhibit no prominent lattice variation. This comparison highlights that it is the H_2O that induces the surface impurity and structure reconstruction, rather than the unstable octahedron mechanism.

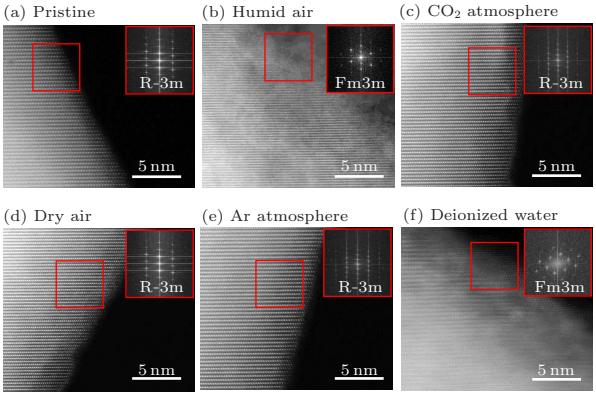

Fig. 3. The STEM images of (a) the pristine NCM811 and the NCM811 stored (b) in humid air for 30 days, (c) in CO_2 for 60 days, (d) in dry air for 1 year, (e) in Ar for 1 year, and (f) after wash with deionized water.

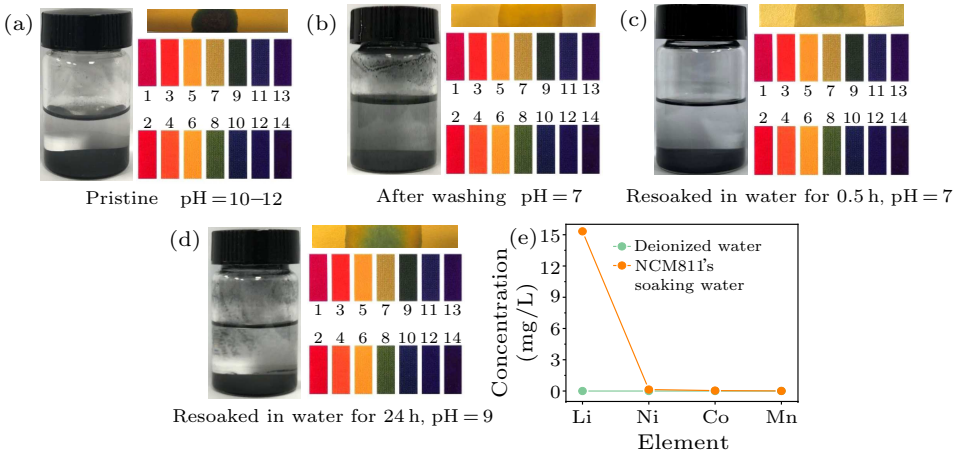

Fig. 4. The pH measurement of NCM811 powder: the pristine NCM811 (a), the NCM811 after washed with deionized water (b), the washed NCM811 re-soaked in water for 30 min (c) and 24 h (d). The ICP results of deionized water and soaking water of the NCM811 (d).

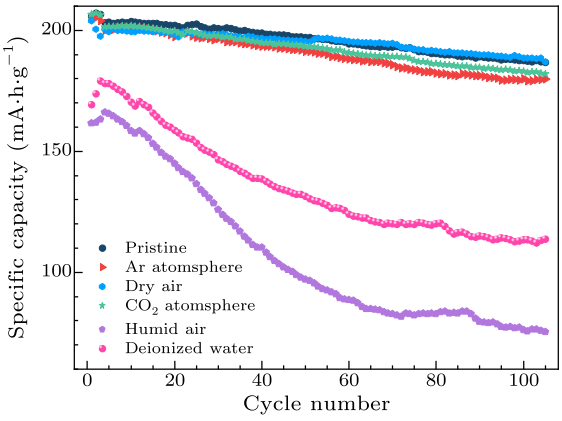

Fig. 5. The cycling performance of NCM811 samples stored in different atmospheres.

To further prove that water causes phase transformation on the surface layer of NCM811, the pH test was carried out on samples with different water washing treatments. As shown in Fig. 4(a), due to the excessive Li source addition in the NCM811 preparation, the pristine sample is alkaline with a pH value of 10–12. After washing for several times, the pH value of soaking water for the NCM811 gradually decreases and reaches 7 [Fig. 4(b)]. Next, the NCM811 soaked in water is dried in vacuum oven. When the dried NCM811 is soaked in water again, the pH value of the suspension is about 7 after 20 min [Fig. 4(c)]. However, the pH value increases to 9 after another 24 hours soaking in water [Fig. 4(d)]. Then the soaking water was separated by centrifugation and filtration, and dissolved in nitric acid for the inductive coupled plasma emission spectrometer (ICP) measurement. As shown in Fig. 4(e), the concentration of Li^+ in the soaking water is 15.32 mg/L, which is much higher than that of pure water (0.0035 mg/L). This is the intuitive evidence of the Li/H exchange happens during storage in the water, as recently supported by Hartmann *et al.*, who also believed that it is

the Li/H exchange that causes the storage instability of the NCM811 in the humid air.[21]

Finally, we investigated the cycling performance of the NCM811 samples stored in different atmospheres. As shown in Fig. 5, the samples that contact moisture (stored in humid air and washed with deionized water) show lower initial discharge capacities, accompanied by the deteriorated cycling stability. This result could be resulted from the formation of the surface reconstruction layer on the NCM811, which consumes active Li and causes poor cycle life.

In summary, we have analyzed the morphology and chemistry of NCM811 samples stored in various atmospheres and found that Li_2CO_3 only generates on the NCM811 surface that is exposed to H_2O and CO_2 simultaneously, and the disordered Li-poor phase is only induced on samples that contact moisture. Therefore, our results support that the surface instability of the NCM811 during storage should be originated from the Li/H exchange mechanism. The viewpoints of this study provide some insights for the development of air stability of NCM811.

References

[1] Li W, Erickson E and Manthiram A 2020 *Nat. Energy* **5** 26
[2] Asif M, Kilian S and Rashad M 2021 *Energy Stor. Mater.* **42** 129
[3] Zhang S, Ma J, Hu Z, Cui G and Chen L 2019 *Chem. Mater.* **31** 6033
[4] Yang L, Yang K, Zheng J, Xu K, Amine K and Pan F 2020 *Chem. Soc. Rev.* **49** 4667
[5] Kim J, Lee H, Cha H, Yoon M, Park M and Cho J 2018 *Adv. Energy Mater.* **8** 1702028
[6] Zhang H and Zhang J 2021 *eTransportation* **7** 100105
[7] Qi X, Liu B, Yun F, Wang C, Wang R, Pang J, Tang H, Quan W, Zhang Q, Yang M, Wu S, Wang J and Sun X 2022 *J. Mater. Chem. A* **10** 1227
[8] Hou P, Yin J, Ding M, Huang J and Xu Y 2017 *Small* **13** 1701802
[9] Cui Z, Xie Q and Manthiram A 2021 *Adv. Energy Mater.* **11** 2102421
[10] You Y, Celio H, Li J, Dolocan A and Manthiram A 2018 *Angew. Chem. Int. Ed.* **130** 6590
[11] Gu W, Dong Q, Zheng L, Liu Y, Mao Y, Zhao Y, Duan W, Lin H, Shen Y and Chen L 2020 *ACS Appl. Mater. Interfaces* **12** 1937
[12] Faenza N V, Bruce L, Lebens-Higgins Z W, Plitz L, Pereira N, Piper L F J and Amatucci G G 2017 *J. Electrochem. Soc.* **164** A3727
[13] Liu H, Yang Y and Zhang J 2006 *J. Power Sources* **162** 644
[14] Martinez A C, Grugeon S, Cailleu D, Courty M, Tran-Van P, Delobel B and Laruelle S 2020 *J. Power Sources* **468** 228204
[15] Kong D, Hu J T, Chen Z, Song K, Li C, Weng M, Li M, Wang R, Liu T, Liu J, Zhang M, Xiao Y and Pan F 2019 *Adv. Energy Mater.* **9** 1901756
[16] Zou L, He Y, Liu Z, Jia H, Zhu J, Zheng J, Wang G, Li X, Xiao J, Zhang J, Chen G and Wang C 2020 *Nat. Commun.* **11** 1
[17] Pritzl D, Teufl T, Freiberg A T S, Strehle B, Sicklinger J, Sommer H, Hartmann P and Gasteiger H A 2019 *J. Electrochem. Soc.* **166** A4056
[18] Hamam I, Zhang N, Liu A, Johnson M and Dahn J 2020 *J. Electrochem. Soc.* **167** 130521
[19] Li J, Li W, You Y and Manthiram A 2018 *Adv. Energy Mater.* **8** 1801957
[20] Duan H, Chen W, Fan M, Wang W, Yu L, Tan S, Chen X, Zhang Q, Xin S, Wan L and Guo Y 2020 *Angew. Chem. Int. Ed.* **59** 12069
[21] Hartmann L, Pritzl D, Beyer H and Gasteiger H A 2021 *J. Electrochem. Soc.* **168** 070507

Supplementary Material: Probing the Air Storage Failure Mechanism of Ni-Rich Layered Cathode Materials

Qingyu Dong(董庆雨)[1#], Ruowei Yi(易若玮)[1#], Jizhen Qi(齐楫真)[1], Yanbin Shen(沈炎宾)[1]*, Liwei Chen(陈立桅)[2]*

[1] i-Lab, CAS Center for Excellence in Nanoscience, Suzhou Institute of Nano-Tech and Nano-Bionics (SINANO), Chinese Academy of Sciences (CAS), Suzhou 215123, China

[2] In Situ Center for Physical Sciences, School of Chemistry and Chemica Engineering, Shanghai Jiaotong University, Shanghai 200240, China

[#] Qingyu Dong. and Ruowei Yi contributed equally to this work.

A. Supplementary data

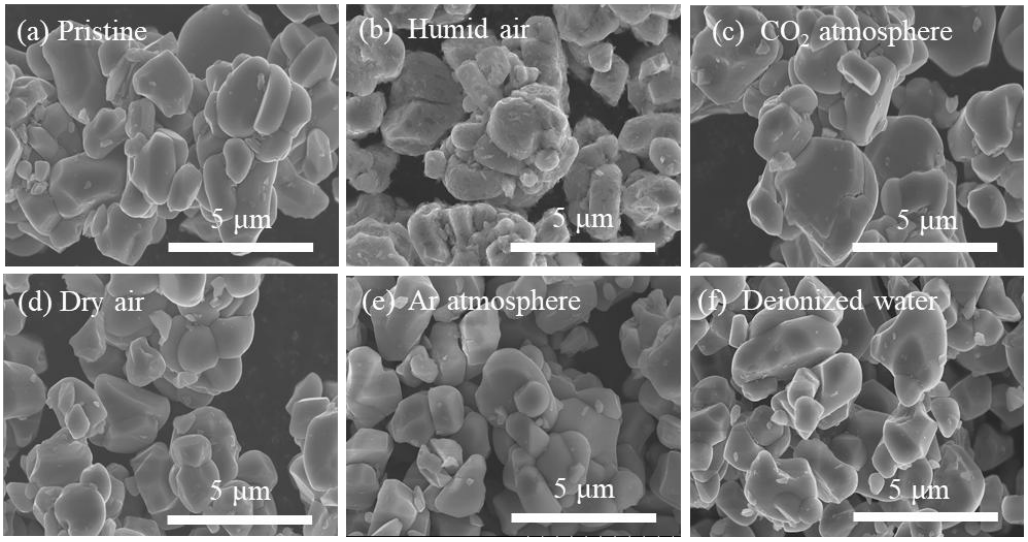

Figure S1. The SEM observation of NCM811 that stored under different atmospheres. (a) The pristine NCM811 and the NCM811 stored in (b) humid air for 30 days, (c) CO_2 for 60 days, (d) dry air for 1 year, (e) Ar for 1 year, and (f) after wash with deionized water.

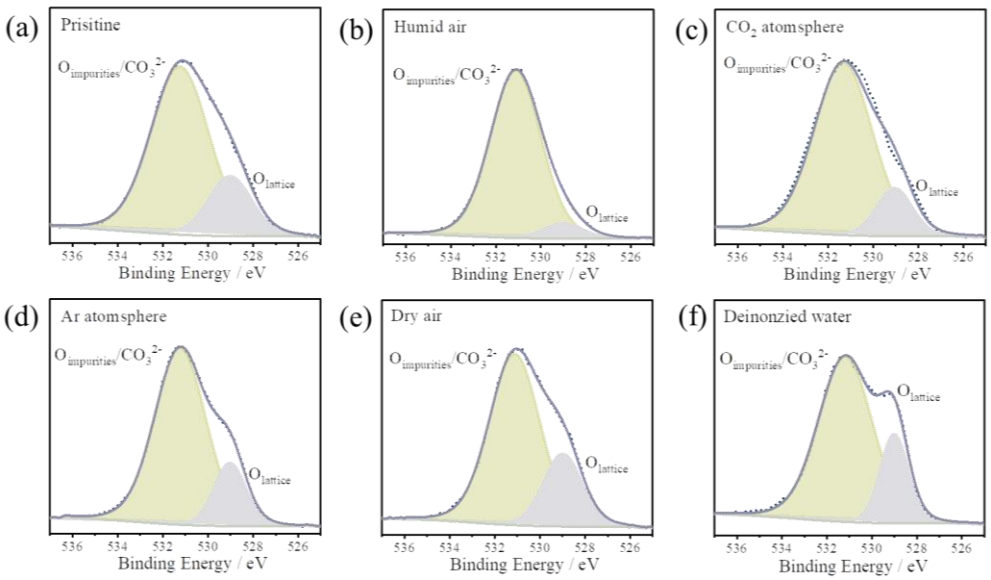

Figure S2. The O 1s XPS of NCM811 samples stored in different atmospheres: (a) the pristine NCM811 and NCM811 stored in (b) humid air for 30 days, (c) CO_2 for 60 days, (d) dry air for 1 year, (e) Ar for 1 year, and (f) after wash with deionized water.

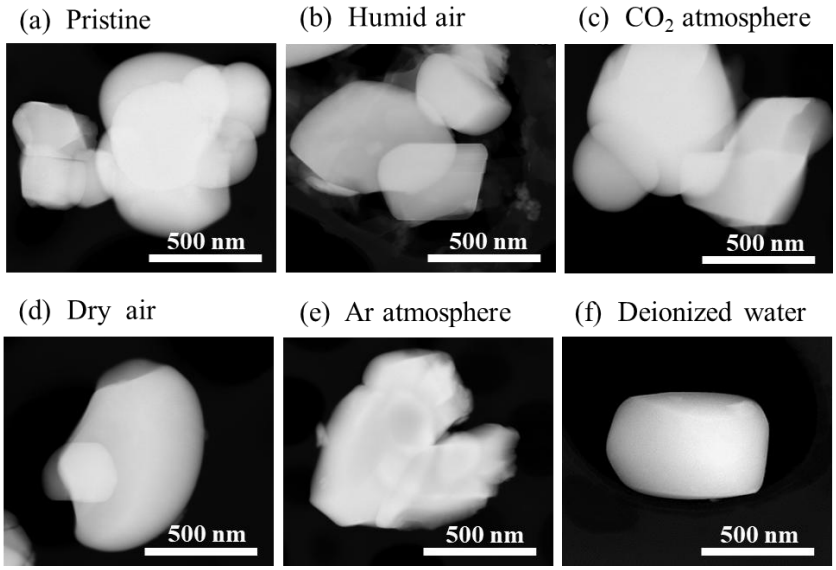

Figure S3. The STEM of NCM811 samples stored in different atmospheres: (a) the pristine NCM811 and NCM811 stored in (b) humid air for 30 days, (c) CO_2 for 60 days, (d) dry air for 1 year, (e) Ar for 1 year, and (f) after wash with deionized water.

B. Sample preparation

The single-crystal Ni-rich layered oxide cathode material used in this work was purchased from Ningbo Ronbay New Energy Technology Co. Ltd., with a chemical composite of $LiNi_{0.83}Co_{0.12}Mn_{0.05}O_2$.

1. Air-storage treatment. The NCM811 was stored outdoors with everyday humidity and temperature recorded, as shown in **Figure** S4. The storage lasted for 30 days. Samples were electrochemically tested and characterized at regular intervals.
2. Water-wash treatment. The NCM811 was soaked in deionized water (degassed and filtered) and washed until the pH value reached 7. Then the water was substituted with anhydrous ethanol ($H_2O \leqslant 50$ ppm, using anhydrous $CuSO_4$ as water indicator). Finally, the sample was vacuum dried. The whole process should ensure the isolation of NCM811 from the air to avoid any $LiOH/Li_2CO_3$ formation on the surface.
3. Special atmosphere storage treatment. The NCM811 was stored in a glove box (no H_2O, CO_2, and O_2), a container filled with pure CO_2, dry-room (dew point = -60 ℃, low H_2O with high O_2 and CO_2) for 1-year, 60-days, and 1-year, respectively.

C. Sample characterizations

SEM characterization: the equipment model is FE-SEM Regulus 8230 (Hitachi, Japan), potential = 10 kV, current = 10 μA.

XPS characterization: the equipment model is PHI 5000 VersaProbe II (Ulvac-PHI, Japan), with a light source of Al kα 1486.6eV and a test area of 100 μm×100 μm.

STEM characterization: the equipment model is FEI Titan Themis Z (Semefi, Japan), with an operating voltage of 300 kV and a current of 60 pA.

ICP was executed using Thermo Fisher Scientific iCAP QC.

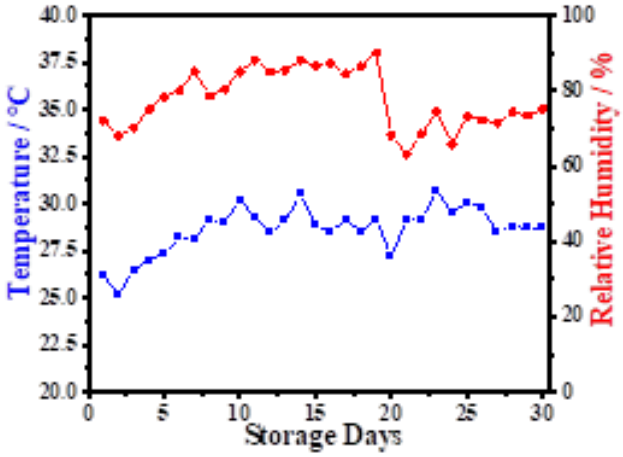

Figure S4. The record of temperature and humidity during the storage of NCM811 in the humid air.